Inorganic Chemistry

Article

pubs.acs.org/IC

Bimetallic Octahedral Ruthenium−Nickel Carbido Cluster Complexes. Synthesis and Structural Characterization

Sumit Saha, Lei Zhu, and Burjor Captain*

Department of Chemistry, University of Miami, Coral Gables, Florida 33124, United States

Supporting Information

ABSTRACT: The reaction of $Ru_5(CO)_{15}(\mu_5\text{-C})$ with $Ni(COD)_2$ in acetonitrile at 80 °C affords the bimetallic octahedral ruthenium−nickel cluster complex $Ru_5Ni(NCMe)(CO)_{15}(\mu_6\text{-C})$, **3**. The acetonitrile ligand in **3** can be replaced by CO and NH_3 to yield $Ru_5Ni(CO)_{16}(\mu_6\text{-C})$, **4**, and $Ru_5Ni(NH_3)(CO)_{15}(\mu_6\text{-C})$, **5**, respectively. Photolysis of compound **3** in benzene and toluene solvent yielded the η^6-coordinated benzene and toluene Ru_5Ni carbido cluster complexes $Ru_5Ni(CO)_{13}(\eta^6\text{-}C_6H_6)(\mu_6\text{-C})$, **6**, and $Ru_5Ni(CO)_{13}(\eta^6\text{-}C_7H_8)(\mu_6\text{-C})$, **7**, respectively. All five new compounds were structurally characterized by single-crystal X-ray diffraction analyses.

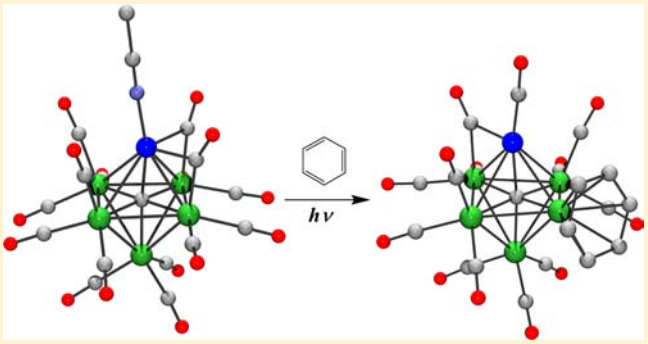

INTRODUCTION

Bimetallic nanoparticle catalysts have been shown to exhibit superior catalytic properties,[1] due to the presence of different metals such that one metal performs a certain role in a catalytic cycle and the other performs another function.[2] Ruthenium-based catalysts modified with group 10 metals have been shown previously to be more active and selective in a number of industrially important hydrogenation processes.[3,4] Supported bimetallic Ru−Ni particles have been of interest in heterogeneous catalysis. For example, it has been shown that the bimetallic cluster $(C_5H_5)NiRu_3H_3(CO)_9$ acts as an effective heterogeneous catalyst for the hydrogenation, dehydrogenation, and isomerization of linear and cyclic monoenes and dienes and aromatic hydrocarbons.[5] The hydrogenation of carbon monoxide was also studied over various titania-supported Ru−Ni bimetallic catalysts.[6] Recently, bimetallic Ru−Ni catalysts are used for steam reforming of ethylene, a key component of biomass derived tars.[7] There is extensive literature on ruthenium complexes containing group 10 elements; however, there are only few examples of ruthenium−nickel complexes.[8−10]

In a previous study, we reported the reaction of $Fe_5(CO)_{15}(\mu_5\text{-C})$ with bis(1,5-cyclooctadiene)nickel(0), $Ni(COD)_2$, in acetonitrile solvent to afford the nickel−iron complex $Fe_5Ni(NCMe)(CO)_{15}(\mu_6\text{-C})$, **1**. Replacement of the acetonitrile ligand with CO gave the binary carbonyl cluster complex $Fe_5Ni(CO)_{16}(\mu_6\text{-C})$, **2**. Additional chemistry with **1** was also studied, which gave new Fe−Ni carbide clusters with varying Fe−Ni ratios.[11]

Herein, we report the reaction of $Ru_5(CO)_{15}(\mu_5\text{-C})$ with $Ni(COD)_2$ in acetonitrile solvent to afford the nickel−ruthenium complex $Ru_5Ni(NCMe)(CO)_{15}(\mu_6\text{-C})$, **3**, and its subsequent reactions with CO and ammonia gas to yield the complexes $Ru_5Ni(CO)_{16}(\mu_6\text{-C})$, **4**, and $Ru_5Ni(NH_3)(CO)_{15}(\mu_6\text{-C})$, **5**, respectively. Furthermore, photolysis of **3** in benzene and toluene solvents furnished the arene coordinated bimetallic cluster complexes $Ru_5Ni(CO)_{13}(\eta^6\text{-}C_6H_6)(\mu_6\text{-C})$, **6**, and $Ru_5Ni(CO)_{13}(\eta^6\text{-}C_7H_8)(\mu_6\text{-C})$, **7**.

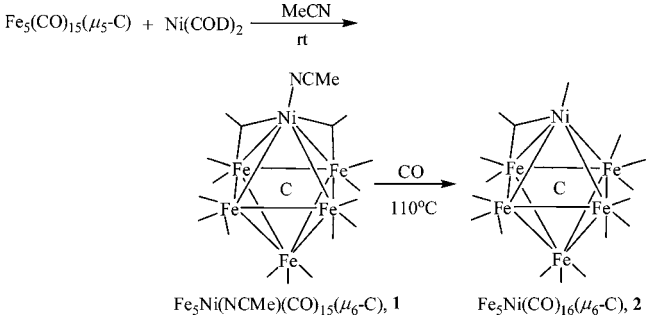

EXPERIMENTAL SECTION

General Data. Unless indicated otherwise, all reactions were performed under an atmosphere of argon. Reagent grade solvents were dried by the standard procedures and were freshly distilled prior to use. Infrared spectra were recorded on a Nicolet 380 FT-IR spectrophotometer. ^{1}H NMR were recorded on a Bruker 400 spectrometer operating at 399.993 MHz. Mass spectrometric measurements performed by a direct-exposure probe using electron impact ionization (EI) were made on a VG 70S instrument at the University of South Carolina, Columbia, South Carolina. Bis(1,5-cyclooctadiene)nickel(0), $Ni(COD)_2$, was purchased from Strem Chemicals, used without further purification, and stored and handled in a drybox. NH_3 was purchased from Matheson Tri-Gas as pure ammonia gas. $Ru_5(CO)_{15}(\mu_5\text{-C})$ was prepared according to the previously published procedure.[12] Product separations were performed by TLC in air on Analtech silica gel GF 250 or 500 μm glass plates. Silica gel (60−200 μm, 70−230 mesh) used for chromatographic separations was purchased from

Received: November 12, 2012
Published: February 19, 2013

   dx.doi.org/10.1021/ic302470w | Inorg. Chem. 2013, 52, 2526−2532

Table 1. Crystallographic Data for Compounds 3−5

	3	4	5
empirical formula	$NiRu_5O_{15}NC_{18}H_3$	$NiRu_5O_{16}C_{17}$	$NiRu_5O_{15}NC_{16}H_3$
formula weight	1037.27	1024.23	1013.25
crystal system	orthorhombic	triclinic	triclinic
lattice parameters			
a (Å)	23.7452(11)	9.2207(4)	9.4325(4)
b (Å)	10.6244(5)	9.9312(4)	17.0113(7)
c (Å)	10.9461(5)	16.0529(7)	17.5226(7)
α (deg)	90	85.1360(6)	62.614(1)
β (deg)	90	83.3197(7)	89.195(1)
γ (deg)	90	63.3268(6)	89.350(1)
V (Å^3)	2761.5(2)	1303.77(10)	2496.27(18)
space group	$Pna2_1$ (No. 33)	$P\bar{1}$ (No. 2)	$P\bar{1}$ (No. 2)
Z value	4	2	4
ρ_{calc} (g/cm^3)	2.495	2.609	2.696
μ (Mo Kα) (mm^{-1})	3.402	3.603	3.760
temp (K)	296	296	296
$2\Theta_{max}$ (deg)	62.00	55.00	56.00
no. obs. ($I > 2\sigma(I)$)	7217	5261	6539
no. parameters	362	352	685
goodness of fit	1.010	1.015	1.097
max. shift in cycle	0.001	0.001	0.001
residuals[a]: R1; wR2	0.0296; 0.0670	0.0321; 0.0840	0.0477; 0.0636
absorption correction	multiscan	multiscan	multiscan
max/min	0.9668/0.3431	0.8693/0.5327	0.7465/0.6478
largest peak in final diff. map (e$^-$/Å^3)	0.805	1.378	0.881

[a] $R = \sum_{hkl}(||F_{obs}| - |F_{calc}||)/\sum_{hkl}|F_{obs}|$; $R_w = [\sum_{hkl}w(|F_{obs}| - |F_{calc}|)^2/\sum_{hkl}wF_{obs}^2]^{1/2}$, $w = 1/\sigma^2(F_{obs})$; GOF $= [\sum_{hkl}w(|F_{obs}| - |F_{calc}|)^2/(n_{data} - n_{vari})]^{1/2}$.

Silicycle. Florisil (F100-500, 60-100 mesh) used for product purifications was purchased from Fisher Scientific.

Preparation of $Ru_5Ni(NCMe)(CO)_{15}(\mu_6\text{-C})$, 3. A 100 mg (0.11 mmol) amount of $Ru_5(CO)_{15}(\mu_5\text{-C})$ and a 40 mg (0.15 mmol) amount of $Ni(COD)_2$ were dissolved in 20 mL of acetonitrile in a 50 mL three-neck round-bottom flask equipped with a reflux condenser. The solution was then heated to reflux with stirring for 15 min, at which time IR showed complete consumption of the starting material, $Ru_5(CO)_{15}(\mu_5\text{-C})$. The solvent was removed *in vacuo*, and the product was separated by column chromatography using a 1:1 hexane/methylene chloride solvent mixture to yield 41 mg (37% yield) of brown $Ru_5Ni(NCMe)(CO)_{15}(\mu_6\text{-C})$, **3**, and a trace amount of $Ru_5(CO)_{15}(\mu_5\text{-C})$. Spectral data for **3**: IR ν_{CO} (cm^{-1} in methylene chloride): 2086 (w), 2045 (s), 2019 (m), 1987 (w, br), 1868 (vw, br). ^{1}H NMR ($CDCl_3$ in ppm): δ = 2.49 (s, 3H, CH_3). EI/MS: m/z 1038 (M^+). The isotope distribution pattern is consistent with the presence of one nickel atom and five ruthenium atoms.

Preparation of $Ru_5Ni(CO)_{16}(\mu_6\text{-C})$, 4. A 50 mg (0.05 mmol) amount of **3** was dissolved in 20 mL of toluene in a 50 mL three-neck round-bottom flask equipped with a reflux condenser. Carbon monoxide gas (1 atm) was bubbled through the solution, and the solution was refluxed at 110 °C with stirring for 15 min, at which time IR showed complete consumption of the starting material **3**. The solvent was removed *in vacuo*, and the product was redissolved in methylene chloride and filtered through florisil to give 48 mg of **4** (97% yield). Spectral data for **4**: IR ν_{CO} (cm^{-1} in hexane): 2104 (vw), 2062 (s), 2050 (m), 2038 (w), 2030 (w), 2001 (w), 1885 (vw, br). EI/MS: m/z 1025 (M^+), 940($M^+ - 3CO$), 912 ($M^+ - 4CO$), 856 ($M^+ - 6CO$). The isotope distribution pattern is consistent with the presence of one nickel atom and five ruthenium atoms.

Preparation of $Ru_5Ni(NH_3)(CO)_{15}(\mu_6\text{-C})$, 5. *Conversion of 3 to 5.* A 20 mg (0.019 mmol) amount of **3** was dissolved in 10 mL of methylene chloride in a 50 mL three-neck round-bottom flask. Ammonia gas (1 atm) was bubbled through the solution, and the solution was stirred at 0 °C (maintained in an ice bath) for approximately 1

Table 2. Crystallographic Data for Compounds 6 and 7

	6	7
empirical formula	$NiRu_5O_{13}C_{20}H_6$	$NiRu_5O_{13}C_{21}H_8$
formula weight	1018.31	1032.33
crystal system	orthorhombic	monoclinic
lattice parameters		
a (Å)	15.3325(6)	17.4209(8)
b (Å)	16.0776(6)	18.8346(8)
c (Å)	21.1873(8)	18.4782(8)
α (deg)	90	90
β (deg)	90	116.945(1)
γ (deg)	90	90
V (Å^3)	5222.9(3)	5404.8(4)
space group	$Pbca$ (No. 61)	$P2_1/n$ (No. 14)
Z value	8	8
ρ_{calc} (g/cm^3)	2.590	2.537
μ (Mo Kα) (mm^{-1})	3.588	3.469
temp (K)	296	296
$2\Theta_{max}$ (deg)	56.00	63.00
no. obs. ($I > 2\sigma(I)$)	5653	13 559
no. parameters	353	723
goodness of fit	1.070	1.036
max. shift in cycle	0.003	0.002
Residuals[a]: R1; wR2	0.0212; 0.0510	0.0320; 0.0762
absorption correction,	multiscan	multiscan
max/min	0.8698/0.3279	0.7688/0.3523
largest peak in final diff. map (e$^-$/Å^3)	0.679	1.631

[a] $R = \sum_{hkl}(||F_{obs}| - |F_{calc}||)/\sum_{hkl}|F_{obs}|$; $R_w = [\sum_{hkl}w(|F_{obs}| - |F_{calc}|)^2/\sum_{hkl}wF_{obs}^2]^{1/2}$, $w = 1/\sigma^2(F_{obs})$; GOF $= [\sum_{hkl}w(|F_{obs}| - |F_{calc}|)^2/(n_{data} - n_{vari})]^{1/2}$.

dx.doi.org/10.1021/ic302470w | Inorg. Chem. 2013, 52, 2526−2532

min, at which time TLC showed complete consumption of the starting material. The reaction solution was filtered through florisil to give 19 mg of **5** (97% yield). Spectral data for **5**: IR ν_{CO} (cm^{-1} in methylene chloride): 2085 (w), 2044 (s), 2019 (m), 1980 (vw, br), 1870 (vw, br). ^1H NMR (CD_2Cl_2 in ppm): δ = 2.95 (s, 3H, NH_3). EI/MS: m/z 1013 (M^+), showing successive loss of eight CO ligands. The isotope distribution pattern is consistent with the presence of one nickel atom and five ruthenium atoms.

*Conversion of **4** to **5**.* A 24 mg (0.023 mmol) amount of **4** was dissolved in 10 mL of methylene chloride in a 50 mL three-neck round-bottom flask. Ammonia gas (1 atm) was then bubbled through the solution, and the solution was stirred at 0 °C (maintained in an ice bath) for approximately 1 min, at which time IR showed complete consumption of the starting material, **4**. The solvent was removed *in vacuo*, and the product was separated on a silica gel column to yield a brown band of **5** (12 mg, 50% yield) eluted by a 1:1 hexane/methylene chloride solvent mixture.

Note: In both cases, the reactions do proceed at room temperature; however, owing to decomposition, the yields at 0 °C are better.

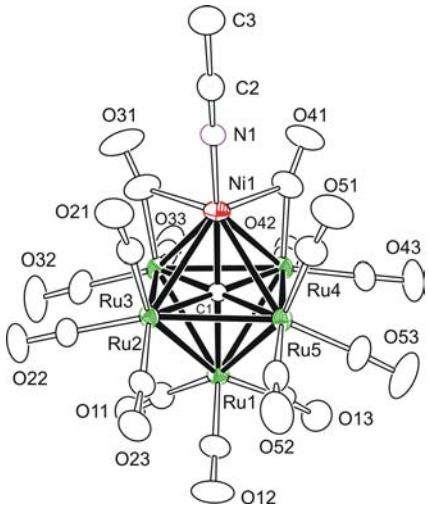

Figure 1. An ORTEP showing the molecular structure of $Ru_5Ni(NCMe)(CO)_{15}(\mu_6\text{-C})$, **3**, with thermal ellipsoids set at 30% probability.

Preparation of $Ru_5Ni(CO)_{13}(\eta^6\text{-}C_6H_6)(\mu_6\text{-C})$, 6 from 3. A 20 mg (0.019 mmol) amount of **3** was dissolved in 20 mL of benzene in a 50 mL three-neck round-bottom flask equipped with a reflux condenser. The solution was irradiated using a high-pressure mercury 1000 W UV lamp (American Ultraviolet Co.) at the 250 wpi (watts per inch) setting for 90 min, at which time IR showed complete consumption of the starting material, **3**. The solvent was removed *in vacuo*, and the product was separated by TLC on silica gel by using a 1:1 hexane/methylene chloride solvent mixture to yield 6.4 mg (33% yield) of green $Ru_5Ni(CO)_{13}(\eta^6\text{-}C_6H_6)(\mu_6\text{-C})$, **6**, and trace amounts of $Ru_5Ni(CO)_{16}(\mu_6\text{-C})$, $Ru_6(CO)_{17}(\mu_6\text{-C})$, $Ru_5(CO)_{15}(\mu_5\text{-C})$, $Ru_5(CO)_{12}(\eta^6\text{-}C_6H_6)(\mu_5\text{-C})$, and $Ru_5Ni(NCMe)(CO)_{15}(\mu_6\text{-C})$. Spectral data for **6**: IR ν_{CO} (cm^{-1} in methylene chloride): 2075 (m), 2043 (vs), 2034 (vs), 2018 (s), 1971 (w), 1853 (vw, br); ^1H NMR (CD_2Cl_2 in ppm): δ = 5.85 (s, 6H, C_6H_6). EI/MS: m/z 1018−1019 (M^+), showing successive loss of 13 CO ligands. The isotope distribution pattern is consistent with the presence of one nickel atom and five ruthenium atoms.

Preparation of $Ru_5Ni(CO)_{13}(\eta^6\text{-}C_6H_6)(\mu_6\text{-C})$, 6, from 4. A 20 mg (0.019 mmol) amount of **4** was dissolved in 20 mL of benzene in a 50 mL three-neck round-bottom flask equipped with a reflux condenser. The solution was irradiated using a high-pressure mercury 1000 W UV lamp (American Ultraviolet Co.) at the 250 wpi setting for 90 min. The solvent was removed *in vacuo*, and the product was separated by TLC on silica gel by using a 1:1 hexane/methylene chloride solvent mixture to yield 5.2 mg (26% yield) of green $Ru_5Ni(CO)_{13}(\eta^6\text{-}C_6H_6)(\mu_6\text{-C})$, **6**.

Preparation of $Ru_5Ni(CO)_{13}(\eta^6\text{-}C_7H_8)(\mu_6\text{-C})$, 7, from 3. A 20 mg (0.019 mmol) amount of **3** was dissolved in 20 mL of toluene in a 50 mL three-neck round-bottom flask equipped with a reflux condenser. The solution was irradiated using a high-pressure mercury 1000 W UV lamp (American Ultraviolet Co.) at the 250 wpi setting for 60 min, at which time IR showed complete consumption of the starting material, **3**. The solvent was removed *in vacuo*, and the product was separated by TLC on silica gel by using a 1:1 hexane/methylene chloride solvent mixture to yield 7.3 mg (37% yield) of green $Ru_5Ni(CO)_{13}(\eta^6\text{-}C_7H_8)(\mu_6\text{-C})$, **7**, and trace amounts of $Ru_5Ni(CO)_{16}(\mu_6\text{-C})$, $Ru_6(CO)_{17}(\mu_6\text{-C})$, $Ru_5(CO)_{15}(\mu_5\text{-C})$, and $Ru_5Ni(MeCN)(CO)_{15}(\mu_6\text{-C})$. Spectral data for **7**: IR ν_{CO} (cm^{-1} in methylene chloride): 2074 (m), 2042 (vs), 2032 (vs), 2017 (s), 1967 (w), 1844 (vw, br); ^1H NMR (CD_2Cl_2 in ppm): δ = 5.80 (d, 2H, CH), 5.75 (t, 2H, CH), 5.67 (t, 1H, CH), 2.38 (s, 3H, CH_3). EI/MS: m/z 1033−1034 (M^+),

Table 3. Selected Intramolecular Distances and Angles for Compounds 3 and 5[a]

atom	atom	distance (Å) **3**	distance (Å) **5**	atom	atom	distance (Å) **3**	distance (Å) **5**
Ni(1)	Ru(2)	2.8394(7)	2.881(1)	Ru(1)	Ru(4)	2.9210(5)	2.870(1)
Ni(1)	Ru(3)	2.6914(7)	2.651(1)	Ru(1)	Ru(5)	2.8420(5)	2.891(1)
Ni(1)	Ru(4)	2.6756(7)	2.706(1)	Ru(2)	Ru(3)	2.9008(5)	2.885(1)
Ni(1)	Ru(5)	2.8831(7)	2.864(1)	Ru(2)	Ru(5)	2.8894(5)	2.891(1)
Ru(1)	Ru(2)	2.8718(5)	2.852(1)	Ru(3)	Ru(4)	2.9103(5)	2.919(1)
Ru(1)	Ru(3)	2.8889(5)	2.909(1)	Ru(4)	Ru(5)	2.8922(5)	2.910(1)
atom		atom	atom		angle (deg) **3**		angle (deg) **5**
Ru(2)		Ni(1)	Ru(3)		63.20(2)		62.71(3)
Ru(2)		Ni(1)	Ru(4)		95.93(2)		94.42(4)
Ru(2)		Ni(1)	Ru(5)		60.65(2)		60.43(3)
Ru(3)		Ni(1)	Ru(4)		65.68(2)		66.02(3)
Ru(3)		Ni(1)	Ru(5)		94.60(2)		96.06(4)
Ru(4)		Ni(1)	Ru(5)		62.57(2)		62.91(3)
Ni(1)		Ru(2)	Ru(3)		55.91(2)		54.73(3)
Ni(1)		Ru(3)	Ru(2)		60.89(2)		62.56(3)
Ni(1)		Ru(3)	Ru(4)		56.90(2)		57.90(3)
Ni(1)		Ru(4)	Ru(3)		57.43(2)		56.08(3)
Ni(1)		Ru(4)	Ru(5)		62.23(2)		61.19(3)
Ni(1)		Ru(5)	Ru(2)		58.93(2)		60.09(3)
Ni(1)		Ru(5)	Ru(4)		55.20(2)		55.90(3)

[a]Estimated standard deviations in the least significant figure are given in parentheses.

dx.doi.org/10.1021/ic302470w | *Inorg. Chem.* 2013, 52, 2526−2532

showing successive loss of nine CO ligands. The isotope distribution pattern is consistent with the presence of one nickel atom and five ruthenium atoms.

Preparation of $Ru_5Ni(CO)_{13}(\eta^6\text{-}C_7H_8)(\mu_6\text{-}C)$, 7, from 4. A 20 mg (0.019 mmol) amount of **4** was dissolved in 20 mL of toluene in a 50 mL three-neck round-bottom flask equipped with a reflux condenser. The solution was irradiated using a high-pressure mercury 1000 W UV lamp (American Ultraviolet Co.) at the 250 wpi setting for 60 min. The solvent was removed *in vacuo*, and the product was separated by TLC on silica gel by using a 1:1 hexane/methylene chloride solvent mixture to yield 2.5 mg (12% yield) of green $Ru_5Ni(CO)_{13}(\eta^6\text{-}C_7H_8)(\mu_6\text{-}C)$, 7.

Crystallographic Analysis. Single crystals of **3**–**7** suitable for diffraction analysis were all grown by slow evaporation of solvent from solutions in a hexane/methylene chloride solvent mixture at −20 °C. The data crystals for **3**–**7** were glued onto the end of a thin glass fiber. X-ray intensity data were measured by using a Bruker SMART APEX2 CCD-based diffractometer using Mo Kα radiation (λ = 0.71073 Å).[13] The raw data frames were integrated with the SAINT+ program by using a narrow-frame integration algorithm.[13] Corrections for Lorentz and polarization effects were also applied with SAINT+. An empirical absorption correction based on the multiple measurement of equivalent reflections was applied using the program SADABS. All structures were solved by a combination of direct methods and difference Fourier syntheses, and refined by full-matrix least-squares on F^2, by using the SHELXTL software package.[14] All non-hydrogen atoms were refined with anisotropic displacement parameters. Hydrogen atoms were placed in geometrically idealized positions and included as standard riding atoms during the least-squares refinements. Crystal data, data collection parameters, and results of the analyses are listed in Tables 1 and 2.

Compound **3** crystallized in the orthorhombic crystal system. The systematic absences in the intensity data were consistent with the space groups *Pnma* and *Pna*2_1. The structure could only be solved in the latter space group. Compounds **4** and **5** crystallized in the triclinic crystal system. The space group $P\bar{1}$ was assumed and confirmed by the successful refinement of the structures. With Z = 4, there are two formula equivalents of complex **5** present in the asymmetric crystal unit. Compound **6** crystallized in the orthorhombic crystal system. The systematic absences in the intensity data were consistent with the unique space group *Pbca*. Compound **7** crystallized in the monoclinic crystal system. The systematic absences in the intensity data were consistent with the unique space group $P2_1/n$. With Z = 8, there are two formula equivalents of the complex present in the asymmetric crystal unit.

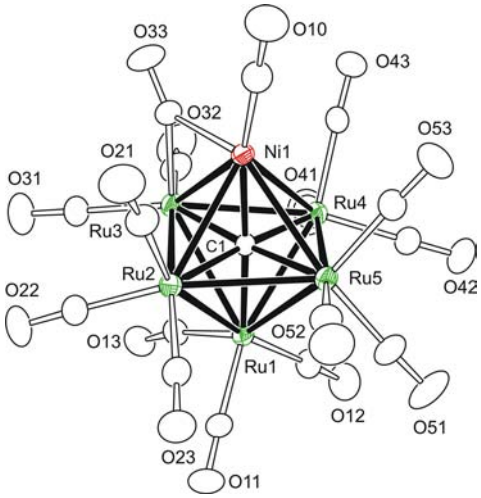

Figure 2. An ORTEP showing the molecular structure of $Ru_5Ni(CO)_{16}(\mu_6\text{-}C)$, **4**, with thermal ellipsoids set at 30% probability.

RESULTS AND DISCUSSION

The bimetallic cluster complex $Ru_5Ni(NCMe)(CO)_{15}(\mu_6\text{-}C)$, **3**, was obtained in 37% yield from the reaction of $Ru_5(CO)_{15}(\mu_5\text{-}C)$, with $Ni(COD)_2$ in acetonitrile solvent under refluxing conditions. Compound **3** was characterized by a combination of IR, ^{1}H NMR, mass spectrometry, and single-crystal X-ray diffraction analyses. An ORTEP showing the molecular structure of **3** is shown in Figure 1. Selected bond distances and angles are listed in Table 3.

Compound **3** is isostructural to the iron analogue cluster **1**, consisting of an octahedron of one nickel atom and five ruthenium atoms. The carbide ligand is encapsulated in the center of the Ru_5Ni octahedron, and the acetonitrile ligand from the reaction solvent is terminally coordinated to the nickel atom. The Ni–carbide distance of 1.862(4) Å is not significantly different from the Ru–carbide distances, which are in the range of 2.033(4)–2.059(4) Å. Also, the Ru–carbide distances are similar to the Ru–carbide distances in $Ru_5(CO)_{15}(\mu_5\text{-}C)$, which are in the range of 2.01(2)–2.10(2) Å. There are two bridging CO ligands, and these bridge the Ni(1)–Ru(3) bond (2.6914(7) Å), and the Ni(1)–Ru(4) bond (2.6756(7) Å). These two metal–metal bonds are shorter than all the other

Table 4. Selected Intramolecular Distances and Angles for Compound 4[a]

atom	atom	distance (Å)	atom	atom	distance (Å)
Ni(1)	Ru(2)	2.8295(6)	Ru(1)	Ru(4)	2.8442(5)
Ni(1)	Ru(3)	2.6624(6)	Ru(1)	Ru(5)	2.9365(5)
Ni(1)	Ru(4)	2.8945(6)	Ru(2)	Ru(3)	2.9384(5)
Ni(1)	Ru(5)	2.8194(6)	Ru(2)	Ru(5)	2.9062(5)
Ru(1)	Ru(2)	2.8541(5)	Ru(3)	Ru(4)	2.9001(5)
Ru(1)	Ru(3)	2.9537(5)	Ru(4)	Ru(5)	2.8682(5)

atom	atom	atom	angle (deg)	atom	atom	atom	angle (deg)
Ru(3)	Ni(1)	Ru(5)	96.16(2)	Ni(1)	Ru(3)	Ru(4)	62.54(2)
Ru(3)	Ni(1)	Ru(2)	64.61(2)	Ni(1)	Ru(3)	Ru(2)	60.45(2)
Ru(5)	Ni(1)	Ru(2)	61.92(2)	Ru(4)	Ru(3)	Ru(2)	89.74(1)
Ru(3)	Ni(1)	Ru(4)	62.76(2)	Ru(5)	Ru(4)	Ni(1)	58.58(1)
Ru(5)	Ni(1)	Ru(4)	60.24(1)	Ru(5)	Ru(4)	Ru(3)	90.04(1)
Ru(2)	Ni(1)	Ru(4)	92.04(2)	Ru(3)	Ru(4)	Ni(1)	54.71(1)
Ni(1)	Ru(2)	Ru(5)	58.87(1)	Ni(1)	Ru(5)	Ru(4)	61.18(2)
Ni(1)	Ru(2)	Ru(3)	54.94(1)	Ni(1)	Ru(5)	Ru(2)	59.21(1)
Ru(5)	Ru(2)	Ru(3)	88.55(1)	Ru(4)	Ru(5)	Ru(2)	91.01(1)

[a]Estimated standard deviations in the least significant figure are given in parentheses.

dx.doi.org/10.1021/ic302470w | *Inorg. Chem.* 2013, 52, 2526–2532

metal−metal bonds, which are in the range of 2.8394(7)−2.9210(5) Å. As expected, compound **3** contains 86 cluster valence electrons, which is in accord with the polyhedral skeletal electron pair theory.[15]

When carbon monoxide gas was purged through solutions of **3** at 110 °C, replacement of the acetonitrile ligand with CO gave the complex $Ru_5Ni(CO)_{16}(\mu_6\text{-C})$, **4**, in 97% yield. Compound **4** was characterized crystallographically, and its molecular structure is shown in Figure 2. Selected bond distances and angles are listed in Table 4.

Compound **4** is isostructural to the known platinum−ruthenium mixed-metal cluster complex $PtRu_5(CO)_{16}(\mu_6\text{-C})$, **8**,[16] that was reported previously, and is isostructural and isomorphous to the Fe_5Ni carbido cluster **2**. Also, as in **8**, one of the metal−metal bonds has a bridging carbonyl group, Ni(1)−Ru(3) = 2.6624(6) Å, which is considerably shorter than all the other metal−metal bonds in **4**.

When solutions of **3** and **4** were exposed to ammonia gas at 0 °C, the complex $Ru_5Ni(NH_3)(CO)_{15}(\mu_6\text{-C})$, **5**, was formed and isolated in 97% and 50% yields, respectively. As in the case with **1** and **2**, both reactions do proceed at room temperature; however, owing to some decomposition, the yields at 0 °C are better. The solid-state structure of **5** is shown in Figure 3, and selected bond distances and angles are listed in Table 3.

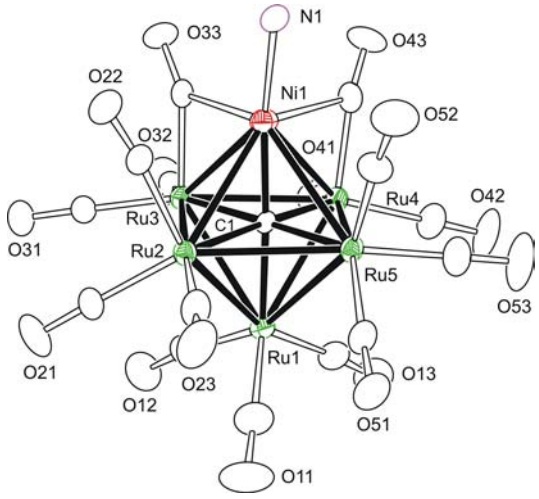

Figure 3. An ORTEP showing the molecular structure of $Ru_5Ni(NH_3)(CO)_{15}(\mu_6\text{-C})$, **5**, with thermal ellipsoids set at 30% probability.

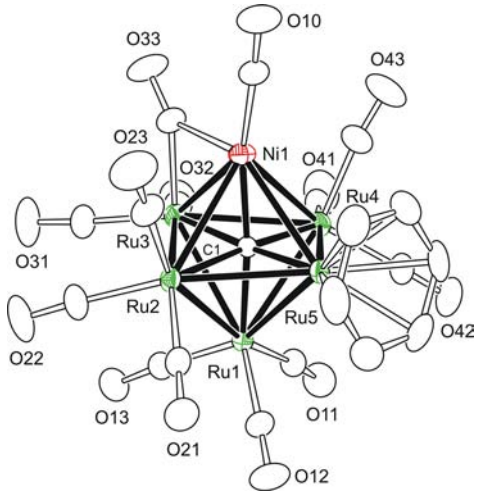

Figure 4. An ORTEP showing the molecular structure of $Ru_5Ni(CO)_{13}(\eta^6\text{-}C_6H_6)(\mu_6\text{-C})$, **6**, with thermal ellipsoids set at 30% probability.

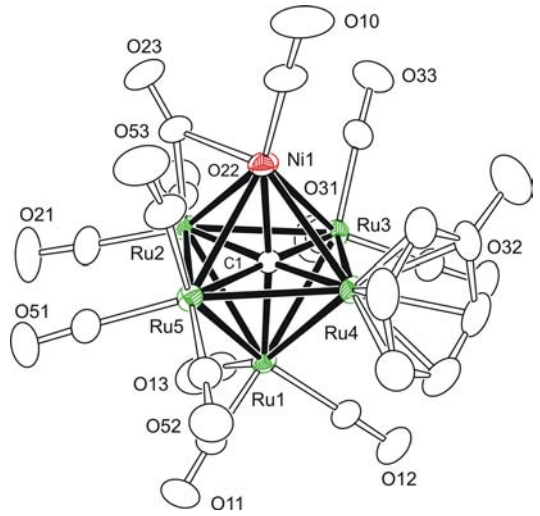

Figure 5. An ORTEP showing the molecular structure of $Ru_5Ni(CO)_{13}(\eta^6\text{-}C_7H_8)(\mu_6\text{-C})$, **7**, with thermal ellipsoids set at 30% probability.

Table 5. Selected Intramolecular Distances and Angles for Compounds 6 and 7[a]

atom	atom	distance (Å) **6**	distance (Å) **7**
Ni(1)	Ru(2)	2.8522(5)	2.6246(5)
Ni(1)	Ru(3)	2.6032(4)	2.8475(6)
Ni(1)	Ru(4)	2.8260(5)	2.7682(5)
Ni(1)	Ru(5)	2.7746(4)	2.7856(6)
Ru(1)	Ru(2)	2.8243(3)	2.9287(4)
Ru(1)	Ru(3)	2.9050(3)	2.8472(4)
Ru(1)	Ru(4)	2.8686(4)	2.8860(4)
Ru(1)	Ru(5)	2.9212(3)	2.8574(4)
Ru(2)	Ru(3)	2.9320(4)	2.8779(4)
Ru(2)	Ru(5)	2.8224(4)	2.8961(4)
Ru(3)	Ru(4)	2.9392(4)	2.8677(4)
Ru(4)	Ru(5)	2.8135(4)	2.8514(4)
atom	atom	atom	angle (deg) **6**	angle (deg) **7**
Ni(1)	Ru(2)	Ru(1)	87.06(1)	89.24(1)
Ni(1)	Ru(2)	Ru(3)	53.473(9)	62.13(1)
Ni(1)	Ru(2)	Ru(5)	58.54(1)	60.37(1)
Ni(1)	Ru(3)	Ru(1)	90.26(1)	86.63(1)
Ni(1)	Ru(3)	Ru(2)	61.69(1)	54.57(1)
Ni(1)	Ru(3)	Ru(4)	60.96(1)	57.94(1)
Ni(1)	Ru(4)	Ru(1)	86.71(1)	87.38(1)
Ni(1)	Ru(4)	Ru(3)	53.64(1)	60.67(1)
Ni(1)	Ru(4)	Ru(5)	58.94(1)	59.41(1)
Ni(1)	Ru(5)	Ru(1)	86.65(1)	87.61(1)
Ni(1)	Ru(5)	Ru(2)	61.27(1)	54.98(1)
Ni(1)	Ru(5)	Ru(4)	60.75(1)	58.81(1)
Ru(2)	Ni(1)	Ru(3)	64.83(1)	63.31(1)
Ru(2)	Ni(1)	Ru(4)	92.96(1)	96.11(1)
Ru(2)	Ni(1)	Ru(5)	60.19(1)	64.65(1)
Ru(3)	Ni(1)	Ru(4)	65.40(1)	61.40(1)
Ru(3)	Ni(1)	Ru(5)	96.23(1)	93.59(1)
Ru(4)	Ni(1)	Ru(5)	60.30(1)	61.78(1)

[a]Estimated standard deviations in the least significant figure are given in parentheses.

dx.doi.org/10.1021/ic302470w | *Inorg. Chem.* 2013, 52, 2526−2532

The structure of compound **5** is similar to that of the iron–nickel cluster complex $Fe_5Ni(NH_3)(CO)_{15}(\mu_6\text{-}C)$ previously reported by us. There are two bridging CO ligands, and these bridge the Ni(1)–Ru(3) bond (2.6506(13) Å), and the Ni(1)–Ru(4) bond (2.7060(14) Å). These two metal–metal bonds are shorter than all the other metal–metal bonds in the octahedral framework, which are in the range of 2.852(1)–2.919(1) Å.

The isolation and characterization of compounds **3**–**5** has proven to be relatively straightforward considering our investigations of the related iron–nickel cluster system. The choice of acetonitrile solvent in the reaction medium is essential to form the Ru_5Ni octahedral framework. It has been shown that $Ru_5(CO)_{15}(\mu_5\text{-}C)$ will readily add small molecules, such as acetonitrile, to yield an open $Ru_5(\mu_5\text{-}C)$ cluster, $Ru_5(CO)_{15}(NCMe)(\mu_5\text{-}C)$, where one ruthenium atom bridges a butterfly arrangement of four other ruthenium atoms.[17] The opening of the $Ru_5(\mu_5\text{-}C)$ cluster facilitates the reaction with $Ni(COD)_2$ by providing vacant coordination sites that are not accompanied by cluster degradation. Migration of the acetonitrile ligand to the nickel atom with subsequent loss of the labile COD groups in $Ni(COD)_2$ gives the parent complex **3**. The iron analogue compound **1** undergoes cluster fragmentation when exposed to UV radiation and heat to form Fe_4Ni and Fe_4Ni_2 carbido clusters. In our efforts to see if, indeed, similar reactivity was observed with the ruthenium–nickel complex **3**, we performed the respective experiments.

When an acetonitrile solution of **3** was heated to reflux, instead of the anticipated five metal, as in the $Fe_4Ni(\mu_5\text{-}C)$ cluster, no reaction was observed. Only when irradiated did we see formation of products. Photolysis of **3** in benzene solvent resulted in the formation of the new complex $Ru_5Ni(CO)_{13}(\eta^6\text{-}C_6H_6)(\mu_6\text{-}C)$, **6**, in 33% yield as the major product. Compound **6** was characterized crystallographically, and its molecular structure is shown in Figure 4.

As seen in Figure 4, compound **6** consists of a $Ru_5Ni(\mu_6\text{-}C)$ cluster where one of the ruthenium vertices is coordinated to a benzene molecule in an η^6- fashion. There are many examples of arene ligands coordinated to metal carbonyl cluster complexes,[18] the first being $Ru_6(CO)_{14}(\eta^6\text{-}C_6H_6)(\mu_6\text{-}C)$ that was reported some years ago. There have also been examples of metal carbonyl clusters to contain bis(arene) ligands and, in some/one case, where a metal cluster is "sandwiched" between two $\eta^6\text{-}C_6H_6$ ligands.[18e,19] However, there have not been many examples of mixed-metal clusters containing the $\eta^6\text{-}C_6H_6$ ligand. The bimetallic complexes that do contain the arene ligand were prepared using an already coordinated benzene ligand in the starting reactant, as seen in the complexes, $Ru_5(CO)_{12}(\eta^6\text{-}C_6H_6)(\mu_6\text{-}C)[PtPBu^t_3]$.[18h,20] In the photolysis reaction of **3**, the complexes $Ru_5Ni(CO)_{16}(\mu_6\text{-}C)$, $Ru_6(CO)_{17}(\mu_6\text{-}C)$, $Ru_5(CO)_{15}(\mu_5\text{-}C)$, $Ru_5(CO)_{12}(\eta^6\text{-}C_6H_6)(\mu_5\text{-}C)$, and $Ru_5Ni(NCMe)(CO)_{15}(\mu_6\text{-}C)$ were also obtained in minor/trace amounts.

Photolysis of a toluene solution of **3** furnished the complex $Ru_5Ni(CO)_{13}(\eta^6\text{-}C_7H_8)(\mu_6\text{-}C)$, **7**, in 37% yield; see Figure 5. Compound **7** is very similar in structure to **6**, where, in place of the benzene ligand, there is now an $\eta^6\text{-}C_7H_8$ group coordinated to one of the ruthenium vertices (Table 5). The $\eta^6\text{-}C_7H_8$ coordination mode has been observed previously in the homometallic carbide cluster $Ru_6(CO)_{14}(\eta^6\text{-}C_7H_8)(\mu_6\text{-}C)$.[18d,21]

The improved synthesis of the various arene coordinated ruthenium carbide clusters is accomplished using cyclohexadiene under thermal conditions or in the presence of trimethylamine *N*-oxide as a decarbonylating reagent to furnish the cyclohexadiene coordinated carbide cluster first, followed by loss of H_2 to yield the benzene coordinated cluster.[18e,f,19a] In our bimetallic system, the arene coordinated complexes **6** and **7**

Scheme 1

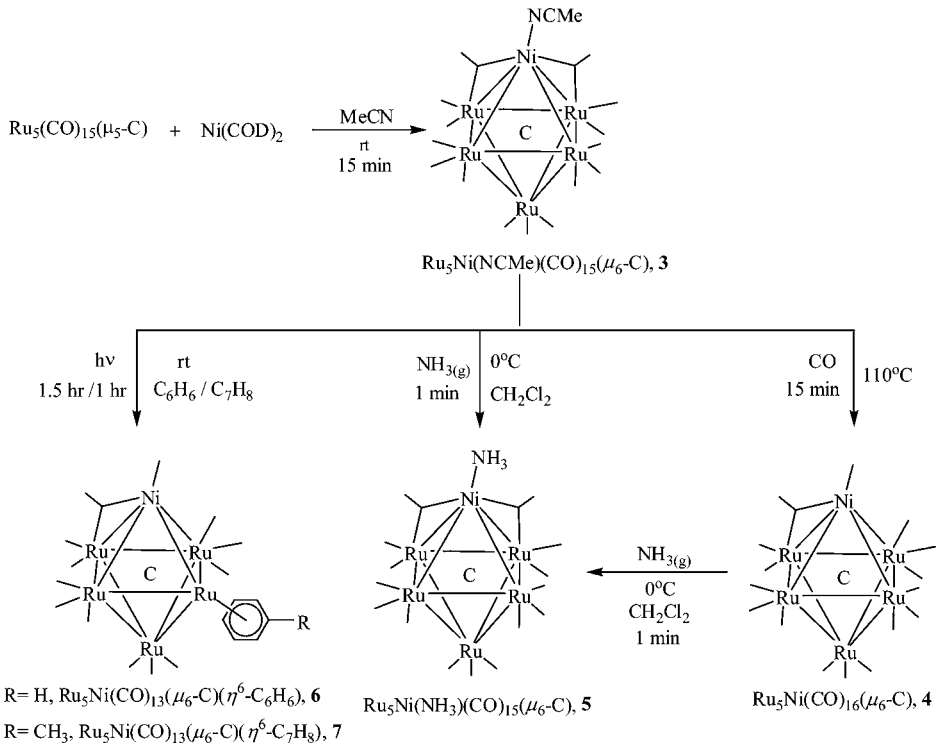

dx.doi.org/10.1021/ic302470w | Inorg. Chem. 2013, 52, 2526–2532

are formed directly from benzene or toluene solvent in reasonable yields under photolytic conditions. Compounds **6** and **7** can also be obtained from the binary cluster **4** under similar conditions.

A series of Ru−Ni carbide cluster complexes have been prepared in reasonable yields, and a summary of the products that were obtained is shown in Scheme 1. The pentaruthenium carbide carbonyl cluster $Ru_5(CO)_{15}(\mu_5\text{-}C)$ reacts with $Ni(COD)_2$ in acetonitrile solvent at room temperature to yield the $NiRu_5$ octahedral cluster, **3**, which has an acetonitrile ligand from the reaction solvent on the nickel atom. The acetonitrile ligand in **3** can be displaced by CO to yield the binary carbonyl cluster complex **4**. Ammonia gas can also replace the acetonitrile ligand in **3** to yield complex **5**. Appropriately, compound **4** can be converted to **5** by reacting with ammonia gas. Photolysis of compound **3** in benzene and toluene solvent afforded η^6-coordinated benzene and toluene Ru_5Ni carbido cluster complexes **6** and **7**, respectively. Studies of some of these compounds to serve as molecular precursors to new nickel−ruthenium nanoparticle catalysts for applications in heterogeneous catalysis are underway.

■ ASSOCIATED CONTENT

Ⓢ Supporting Information

CIF files for each of the structural analyses. This material is available free of charge via the Internet at http://pubs.acs.org.

■ AUTHOR INFORMATION

Corresponding Author

*E-mail: Captain@miami.edu.

Notes

The authors declare no competing financial interest.

■ REFERENCES

(1) (a) Sinfelt, J. H. *Bimetallic Catalysts: Discoveries, Concepts and Applications*; Wiley: New York, 1983. (b) Sachtler, W. M. H. *J. Mol. Catal.* **1984**, *25*, 1−12.

(2) (a) Goodman, D. W.; Houston, J. E. *Science* **1987**, *236*, 403−409. (b) Ichikawa, M. *Adv. Catal.* **1992**, *38*, 283−400.

(3) Raja, R.; Khimyak, T.; Thomas, J. M.; Hermans, S.; Johnson, B. F. G. *Angew. Chem., Int. Ed.* **2001**, *40*, 4638−4642.

(4) Raja, R.; Sankar, G.; Hermans, S.; Shephard, D. S.; Bromley, S.; Thomas, J. M.; Johnson, B. F. G.; Maschmeyer, T. *Chem. Commun.* **1999**, 1571−1572.

(5) Castiglioni, M.; Giordano, R.; Sappa, E. *J. Mol. Catal.* **1987**, *40*, 65−69.

(6) Das, P. C.; Pradhan, N. C.; Dalai, A. K.; bakshi, N. N. *Fuel Process. Technol.* **2004**, *85*, 1487−1501.

(7) Rangan, M.; Yung, M. M. *Catal. Lett.* **2012**, *142*, 718−727.

(8) Khimyak, T.; Johnson, B. F. G. *J. Cluster Sci.* **2004**, *15*, 543−558.

(9) Lanfranchi, M.; Tiripicchio, A.; Sappa, E.; Carty, A. J. *J. Chem. Soc., Dalton Trans.* **1986**, 2737−2740.

(10) Brivio, E.; Ceriotti, A.; Della Pergola, R.; Garlaschelli, L.; Manassero, M.; Sansoni, M. *J. Cluster Sci.* **1995**, *6*, 271−287.

(11) Saha, S.; Zhu, L.; Captain, B. *Inorg. Chem.* **2010**, *49*, 3465−3472.

(12) Nicholls, J. N.; Vargas, M. D.; Hriljac, J.; Sailor, M. *Inorg. Synth.* **1989**, *26*, 283.

(13) *Apex2*, Version 2.2-0, and *SAINT+*, Version 7.46A; Bruker Analytical X-ray System, Inc.: Madison, WI, 2007.

(14) (a) Sheldrick, G. M. *SHELXTL*, Version 6.1; Bruker Analytical X-ray Systems, Inc.: Madison, WI, 2000. (b) Sheldrick, G. M. *Acta Crystallogr.* **2008**, *A64*, 112−122.

(15) (a) Mingos, D. M. P. *Acc. Chem. Res.* **1984**, *17*, 311−319. (b) Mingos, D. M. P. *Introduction to Cluster Chemistry*; Prentice Hall: Engelwood Cliffs, NJ, 1990; Chapter 2.

(16) Adams, R. D.; Wu, W. *J. Cluster Sci.* **1991**, *2*, 271−290.

(17) (a) Johnson, B. F. G.; Lewis, J.; Nicholls, J. N.; Oxton, I. A.; Raithby, P. J.; Rosales, M. J. *Chem. Commun.* **1982**, 289−290. (b) Dyson, P. J. *Adv. Organomet. Chem.* **1998**, *43*, 43−124.

(18) (a) Johnson, B. F. G.; Lewis, J.; Williams, I. G. *J. Chem. Soc. A* **1968**, 2865. (b) Eady, C. R.; Johnson, B. F. G.; Lewis, J. *J. Chem. Soc., Dalton Trans.* **1975**, 2606. (c) Braga, D.; Grepioni, F.; Righi, S.; Dyson, P. J.; Johnson, B. F. G.; Bailey, P. J.; Lewis, J. *Organometallics* **1992**, *11*, 4042−4048. (d) Dyson, P. J.; Johnson, B. F. G.; Reed, D.; Braga, D.; Grepioni, F.; Parisini, E. *J. Chem. Soc., Dalton Trans.* **1993**, 2817−2815. (e) Dyson, P. J.; Johnson, B. F. G.; Lewis, J.; Martinelli, M.; Braga, D.; Grepioni, F. *J. Am. Chem. Soc.* **1993**, *115*, 9062−9068. (f) Braga, D.; Grepioni, F.; Sabatino, P.; Dyson, P. J.; Johnson, B. F. G.; Lewis, J.; Bailey, P. J.; Raithby, P. R.; Stalke, D. *J. Chem. Soc., Dalton Trans.* **1993**, 985−992. (g) Bailey, P. J.; Braga, D.; Dyson, P. J.; Grepioni, F.; Johnson, B. F. G.; Lewis, J.; Sabatino, P. *Chem. Commun.* **1992**, 177−178. (h) Wing-Sze Hui, J.; Wong, W.-T. *J. Organomet. Chem.* **1996**, *524*, 211−217. (i) Mallors, R. L.; Blake, A. J.; Parsons, S.; Johnson, B. F. G.; Dyson, P. J.; Braga, D.; Grepioni, F.; Parisini, E. *J. Organomet. Chem.* **1997**, *532*, 133−142.

(19) (a) Adams, R. D.; Wu, W. *Polyhedron* **1992**, *11*, 2123−2124. (b) Gomez-Sal, M. P.; Johnson, B. F. G.; Lewis, J.; Raithby, P. R.; Wright, A. H. *Chem. Commun.* **1985**, 1682−1684. (c) Dyson, P. J.; Johnson, B. F. G.; Lewis, J.; Braga, D.; Sabatino, P. *Chem. Commun.* **1993**, 301−302. (d) Braga, D.; Sabatino, P.; Dyson, P. J.; Blake, A. J.; Johnson, B. F. G. *J. Chem. Soc., Dalton Trans.* **1994**, 393−399.

(20) (a) Adams, R. D.; Captain, B.; Pellechia, P. J.; Zhu, L. *Inorg. Chem.* **2004**, *43*, 7243−7249. (b) Adams, R. D.; Captain, B.; Fu, W.; Hall, M. B.; Manson, J.; Smith, M. D.; Webster, C. E. *J. Am. Chem. Soc.* **2004**, *126*, 5253−5267.

(21) (a) Farrugia, L. J. *Acta Crystallogr., Sect.C: Cryst. Struct. Commun.* **1988**, *44*, 997−998. (b) Dyson, P. J.; Johnson, B. F. G.; Braga, D.; Grepioni, F.; Martin, C. M.; Parisini, E. *Inorg. Chim. Acta* **1995**, *235*, 413−420. (c) Braga, D.; Grepioni, F.; Parisini, E.; Dyson, P. J.; Johnson, B. F. G.; Reed, D.; Shepherd, D. S.; Bailey, P. J.; Lewis, J. *J. Organomet. Chem.* **1993**, *462*, 301−308.